First publ. in: Optics Express ; 20 (2012), 25. - S. 27456-27464

Mid-infrared optical parametric amplifier based on a LGSe crystal and pumped at 1.6 μm.

Etienne Pelletier,[1] Alexander Sell,[3,4] Alfred Leitenstorfer,[4] and RJ Dwayne Miller[1,2,*]

[1]*Departments of Chemistry and Physics, University of Toronto 80 St. George Street, Toronto, Ontario M5S 3H6, Canada*
[2]*Max Planck Department for Structural Dynamics, Department of Physics, University of Hamburg Centre for Free Electron Laser Science, DESY Notkestrasse 85, Hamburg 22607, Germany*
[3]*TOPTICA Photonics AG Lochhamer Schlag 19, 82166 Graefelfing, Germany*
[4]*Department of Physics and Center for Applied Photonics, University of Konstanz 78464 Konstanz, Germany*

[*]*dwayne.miller@mpsd.cfel.de*

Abstract: We demonstrate the generation of 22.6 μJ of combined energy at 3 μm for sub-300fs pulses at a repetition rate of 1 kHz using a LGSe optical parametric amplifier (OPA). The LGSe OPA is pumped by the 140-fs 1.6 μm pulses from a 300-mW KTA optical parametric chirped pulse amplifier (OPCPA) based on an all-optical synchronization scheme. By using a highly-nonlinear fiber, the output of an erbium-doped fiber laser operating at 1560 nm is shifted to 1050 nm in order to coherently seed a Nd:YLF regenerative amplifier. The LGSe OPA is seeded using the MIR coming from the amplification of the 1.6 μm in the OPCPA .

OCIS codes: (140.3070) Infrared and far-infrared lasers; (140.7090) Ultrafast lasers; (190.4970) Parametric oscillators and amplifiers; (190.4370) Nonlinear optics, fibers.

References and links

1. S. Woutersen, U. Emmerichs, and H. Bakker, "Femtosecond mid-IR pump-probe spectroscopy of liquid water: Evidence for a two-component structure," Science **278**, 658–660 (1997).
2. P. Hamm, M. Lim, and R. Hochstrasser, "Non-Markovian dynamics of the vibrations of ions in water from femtosecond infrared three-pulse photon echoes," Phys. Rev. Lett. **81**, 5326–5329 (1998).
3. M. Cowan, B. Bruner, N. Huse, J. Dwyer, B. Chugh, E. Nibbering, T. Elsaesser, and R. Miller, "Ultrafast memory loss and energy redistribution in the hydrogen bond network of liquid H_2O," Nature **434**, 199–202 (2005).
4. L. Szyc, J. R. Dwyer, E. T. J. Nibbering, and T. Elsaesser, "Ultrafast dynamics of N-H and O-H stretching excitations in hydrated DNA oligomers," Chem. Phys. **357**, 36–44 (2009).
5. K. Ramasesha, S. T. Roberts, R. A. Nicodemus, A. Mandal, and A. Tokmakoff, "Ultrafast 2D IR anisotropy of water reveals reorientation during hydrogen-bond switching," J. Chem. Phys. **135**, 054509 (2011).
6. P. Hamm, R. Kaindl, and J. Stenger, "Noise suppression in femtosecond mid-infrared light sources," Opt. Lett. **25**, 1798–1800 (2000).
7. R. Kaindl, M. Wurm, K. Reimann, P. Hamm, A. Weiner, and M. Woerner, "Generation, shaping, and characterization of intense femtosecond pulses tunable from 3 to 20 μm," J. Opt. Soc. Am. B **17**, 2086–2094 (2000).
8. F. Morin, F. Druon, M. Hanna, and P. Georges, "Microjoule femtosecond fiber laser at 1.6 μm for corneal surgery applications," Opt. Lett. **34**, 1991–1993 (2009).
9. D. Herrmann, L. Veisz, R. Tautz, F. Tavella, K. Schmid, V. Pervak, and F. Krausz, "Generation of sub-three-cycle, 16 TW light pulses by using noncollinear optical parametric chirped-pulse amplification," Opt. Lett. **34**, 2459–2461 (2009).

#175727 - $15.00 USD Received 10 Sep 2012; revised 19 Oct 2012; accepted 23 Oct 2012; published 26 Nov 2012

10. J. Rudd, R. Law, T. Luk, and S. Cameron, "High-power optical parametric chirped-pulse amplifier system with a 1.55 μm signal and a 1.064 μm pump," Opt. Lett. **30**, 1974–1976 (2005).
11. D. Kraemer, M. L. Cowan, R. Hua, K. Franjic, and R. D. Miller, "High-power femtosecond infrared laser source based on noncollinear optical parametric chirped pulse amplification," J. Opt. Soc. Am. B **24**, 813–818 (2007).
12. O. Chalus, A. Thai, P. K. Bates, and J. Biegert, "Six-cycle mid-infrared source with 3.8 μJ at 100 kHz," Opt. Lett. **35**, 3204–3206 (2010).
13. C. Heese, C. R. Phillips, L. Gallmann, M. M. Fejer, and U. Keller, "Ultrabroadband, highly flexible amplifier for ultrashort midinfrared laser pulses based on aperiodically poled Mg:$LiNbO_3$," Opt. Lett. **35**, 2340–2342 (2010).
14. X. Gu, G. Marcus, Y. Deng, T. Metzger, C. Teisset, N. Ishii, T. Fuji, A. Baltuska, R. Butkus, V. Pervak, H. Ishizuki, T. Taira, T. Kobayashi, R. Kienberger, and F. Krausz, "Generation of carrier-envelope-phase-stable 2-cycle 740-μJ pulses at 2.1-μm carrier wavelength," Opt. Express **17**, 62–69 (2009).
15. G. Andriukaitis, T. Balciunas, S. Alisauskas, A. Pugzlys, A. Baltuska, T. Popmintchev, M.-C. Chen, M. M. Murnane, and H. C. Kapteyn, "90 GW peak power few-cycle mid-infrared pulses from an optical parametric amplifier," Opt. Lett. **36**, 2755–2757 (2011).
16. R. Shelton, S. Foreman, L. Ma, J. Hall, H. Kapteyn, M. Murnane, M. Notcutt, and J. Ye, "Subfemtosecond timing jitter between two independent, actively synchronized, mode-locked lasers," Opt. Lett. **27**, 312–314 (2002).
17. K.-H. Hong, S.-W. Huang, J. Moses, X. Fu, C.-J. Lai, G. Cirmi, A. Sell, E. Granados, P. Keathley, and F. X. Kaertner, "High-energy, phase-stable, ultrabroadband kHz OPCPA at 2.1 μm pumped by a picosecond cryogenic Yb:YAG laser," Opt. Express **19**, 15538–15548 (2011).
18. C. Teisset, N. Ishii, T. Fuji, T. Metzger, S. Kohler, R. Holzwarth, A. Baltuska, A. Zheltikov, and F. Krausz, "Soliton-based pump-seed synchronization for few-cycle OPCPA," Opt. Express **13**, 6550–6557 (2005).
19. F. Adler, A. Sell, F. Sotier, R. Huber, and A. Leitenstorfer, "Attosecond relative timing jitter and 13 fs tunable pulses from a two-branch Er:fiber laser," Opt. Lett. **32**, 3504–3506 (2007).
20. A. Sell, G. Krauss, R. Scheu, R. Huber, and A. Leitenstorfer, "8-fs pulses from a compact Er:fiber system: quantitative modeling and experimental implementation," Opt. Express **17**, 1070–1077 (2009).
21. S. Kumkar, G. Krauss, M. Wunram, D. Fehrenbacher, U. Demirbas, D. Brida, and A. Leitenstorfer, "Femtosecond coherent seeding of a broadband Tm:fiber amplifier by an Er:fiber system," Opt. Lett. **37**, 554–556 (2012).
22. R. Stolen and C. Lin, "Self-phase-modulation in silica optical fibers," Phys. Rev. A **17**, 1448–1453 (1978).
23. S. Witte, R. Zinkstok, A. Wolf, W. Hogervorst, W. Ubachs, and K. Eikema, "A source of 2 terawatt, 2.7 cycle laser pulses based on noncollinear optical parametric chirped pulse amplification," Opt. Express **14**, 8168–8177 (2006).
24. L. Isaenko, A. Yelisseyev, S. Lobanov, P. Krinitsin, V. Petrov, and J. J. Zondy, "Ternary chalcogenides $LiBC_2$ (B = In, Ga; C=S, Se, Te) for mid-IR nonlinear optics," J. Non-Cryst. Solids **352**, 2439–2443 (2006). 1st Conference on Advances in Optical Materials (AIOM), Tucson, AZ, OCT 12-15, 2005.
25. T. Elsaesser, A. Seilmeier, W. Kaiser, P. Koidl, and G. Brandt, "Parametric generation of tunable picosecond pulses in the medium infrared using aggas2 crystal," Appl. Phys. Lett. **44**, 383–385 (1984).
26. T. Kobayashi and A. Shirakawa, "Tunable visible and near-infrared pulse generator in a 5 fs regime," Appl. Phys. B-Laser O. **70**, S239–S246 (2000). Ultrafast Optics 1999 Meeting, Ctr, Stefano Franscini, Ascona, Switzerland, July 12-16, 1999.
27. X. 'Fu, Q. Liu, X. Yan, J. Cui, and M. Gong, "1 mJ, 500 kHz Nd:YAG/Nd:YVO_4 MOPA laser with a Nd:YAG cavity-dumping seed laser," Laser Phys. **20**, 1707–1711 (2010).
28. M. Schulz, R. Riedel, A. Willner, T. Mans, C. Schnitzler, P. Russbueldt, J. Dolkemeyer, E. Seise, T. Gottschall, S. Haedrich, S. Duesterer, H. Schlarb, J. Feldhaus, J. Limpert, B. Faatz, A. Tuennermann, J. Rossbach, M. Drescher, and F. Tavella, "Yb:YAG innoslab amplifier: efficient high repetition rate subpicosecond pumping system for optical parametric chirped pulse amplification," Opt. Lett. **36**, 2456–2458 (2011).

1. Introduction

Recent advances in ultrafast mid-infrared (MIR, 2-20 μm) spectroscopy have made it possible to probe structural dynamics [1–5] on the sub-picosecond time scale. With increasing peak powers, processes can be driven far from equilibrium allowing strong field control and eventually laser selective chemistry. However, generating short laser pulses at those frequencies is rather difficult because of a lack of suitable laser media and the broad frequency range needed. Furthermore, a relatively high repetition rate (kHz and up) is needed to obtain acceptable signal-to-noise for the observables of interest. To date, most ultrafast MIR systems are based on optical parametric amplifiers (OPAs) pumped by a Ti:Sapphire laser at 800 nm [6, 7]. However, the comparatively short wavelength of Ti:Sapphire puts harsh requirements on the nonlinear crystals with respect to optical damage through low number, 2-3 photon, absorption at the required peak power for nonlinear generation of IR. Therefore MIR-light generation with Ti:Sapphire

#175727 - $15.00 USD Received 10 Sep 2012; revised 19 Oct 2012; accepted 23 Oct 2012; published 26 Nov 2012

systems is often achieved through two subsequent nonlinear processes. This reduces the overall efficiency and makes scalability difficult. Using longer pump wavelengths would result in less stringent requirements for the OPA crystals with respect to damage thresholds related to multiphoton processes, opening the door to new and simpler designs.

Erbium-doped fiber lasers (EDFLs) operating at 1.55 μm are widely available. They are an attractive alternative for ultrafast laser systems as they are truly turn-key and extremely robust against cavity misalignment. However, with EDFL systems, it is difficult to reach multi-μJ level while keeping the bandwidth needed for 100-fs pulses [8]. Optical parametric chirped-pulse amplification can generate high gain for large bandwidth at arbitrary wavelengths. It has been used widely in conjunction with Ti:Sapphire lasers and has produced few-cycle pulses with energy in the mJ range [9]. In recent years, OPCPA systems have also been developed for longer wavelengths [10–15]. Furthermore the amplification of 1.6 μm light by 1 μm generates an idler at 3 μm. However, in the noncollinear geometry, the idler is angularly dispersed and temporally stretched and is not usable right away. Previous work [15] has used a collinear geometry to avoid this problem as well as changing the stretcher design to allow the idler to be recompressed using a simple two-grating compressor. This solution is attractive but offers little tunability. Using an OPA pumped by the compressed output of the OPCPA is an alternative. As a proof-of-principle, the idler of the OPCPA can be used as the seed if the angular chirp is removed, but because of the inherent flexibility of the system, white light seeding is also possible, offering a greater tunability.

In the first part of this article we report the performance of a potassium titanyl arsenate ($KTiOAsO_4$ - KTA) OPCPA based on an EDFL and an all-optical synchronization scheme. In the second part, a MIR OPA based on a lithium gallium selenide ($LiGaSe_2$ - LGSe) crystal is demonstrated. This OPA is pumped by the compressed output of the OPCPA and seeded by its idler. However, as the idler has an angular frequency chirp, it has to be conditioned before being sent to the OPA.

2. Passively-synchronized optical parametric chirped pulse amplifier

One of the main drawbacks of the OPCPA concept is the need for low timing jitter between the pump and the seed. One way to solve this problem is to use electronic synchronization based on phase-locked loops. The technology is becoming mature and has showed great success; less than 1-fs jitters have been reported [16]. Although phase-locked loops can be quite good, actively stabilized systems are inherently unstable and require constant monitoring and adjusting. In contrast, all-optical synchronization schemes are passive, depending only on the stability of the optomechanical system and environment, which can be made sufficiently robust to enable reproducible use on a daily basis. The idea of passive synchronization has been around since the early days of OPCPAs and has been implemented in different ways with Ti:Sapphire (e.g. [17, 18]). However, as good as they are, Ti:Sapphire systems are expensive and extremely sensitive to misalignment. In addition, as mentioned above, there is the limitation in power scaling in the MIR region. A different scheme relying on an Ytterbium solid-state amplifier was used by Baltuska et al. [15] and shows great promise. For our system, we explore a different direction and are using a low-power erbium-doped fiber system as a synchronized source for OPCPA which has the advantages of greater simplicity, lower cost, and robustness against misalignment.

2.1. Experimental setup

The schematic of the OPCPA is illustrated in fig 1. The oscillator, for both the seed and the pump arm, is a commercial EDFL (Calmar laser) delivering 0.5 nJ 100-fs pulses at 1.56 μm with a repetition rate of 20 MHz. The output is divided in two and seeded to two separate

#175727 - $15.00 USD Received 10 Sep 2012; revised 19 Oct 2012; accepted 23 Oct 2012; published 26 Nov 2012

homemade erbium-doped fiber amplifiers (EDFAs). Each amplifier consists of a 3m-long 4-μm core 80-dB erbium-doped fiber (Liekki Er80-4/125) pumped at both ends by 980-nm 300 mW laser diodes (JDSU 27-8052-300). The pulses are amplified to 2 nJ and their duration reduced to 80-fs by the combined effects of the anomalous dispersion in the erbium-doped fiber and self-phase modulation in the amplifier. The output of one of the two amplifiers is coupled out of the fiber and sent to a Martinez-type reflective grating stretcher (750 lines/mm gold grating). In a double pass configuration, the pulses are stretched to 50-ps and sent to the OPCPA.

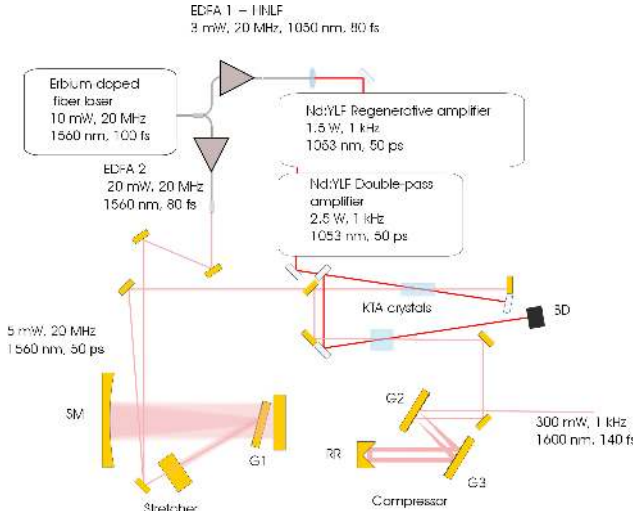

Fig. 1. The OPCPA layout. Detailed description of each part can be found in the text. EDFA, erbium-doped fiber amplifier; HNLF, highly nonlinear fiber; G1, G2, G3, gratings; SM, spherical mirror; RR, retroreflector; BD, beam dump.

The output of the second amplifier is coupled to a highly-nonlinear fiber (HNLF) [19] to generate the 1-μm light needed to seed the OPCPA pump laser. A 80-mm precompression fiber (PF) is spliced to a HNLF, which is a 140-mm small-core germano-silicate fiber. As the pulses enter the PF, they are undergoing solitonic compression. The length of the fiber is chosen to minimize the pulse duration before they go into the HNLF where the 1 μm needed for seeding the regenerative amplifier is generated through soliton fission and four-wave mixing (see [20] for a detailed explanation). By selecting the correct dispersion of the fiber and adjusting the prechirp of the pump it is possible to optimize the power generated at 1 μm [20]. The dispersion profiles for the PF and the HNLF are shown in Fig. 2. Previous work has shown that the timing jitter introduced by the frequency shifting with this kind of HNLF is in the attosecond regime [19] and there is no loss of first-order coherence [21]. The fiber output power is 3 mW and the bandwidth is 50 nm centered at 1050 nm (see Fig. 2).

The output of the HNLF is sent to a homebuilt Nd:YLF regenerative amplifier pumped by 120 W diode lasers (Cutting Edge laser module RBA30-1C2). However, because Nd:YLF has a bandwidth of only 1.1 nm, the regenerative amplifier is effectively seeded with roughly 1 pJ. This bandwidth restriction combined with gain narrowing results in 15-ps output pulses for moderate amplification. To avoid damaging optics during the amplification, two etalons (1 mm and .75 mm) are introduced into the regen cavity to stretch the pulse to 50 ps. The amplifier output power is 1.5 W at 1 kHz. The output shot-to-shot fluctuation was measured to be less than 0.5% (1 standard deviation for 256 pulses). Before going to the OPCPA, the pump pulses are sent to a homebuilt double-pass Nd:YLF amplifier (based on a Cutting Edge laser module

#175727 - $15.00 USD Received 10 Sep 2012; revised 19 Oct 2012; accepted 23 Oct 2012; published 26 Nov 2012

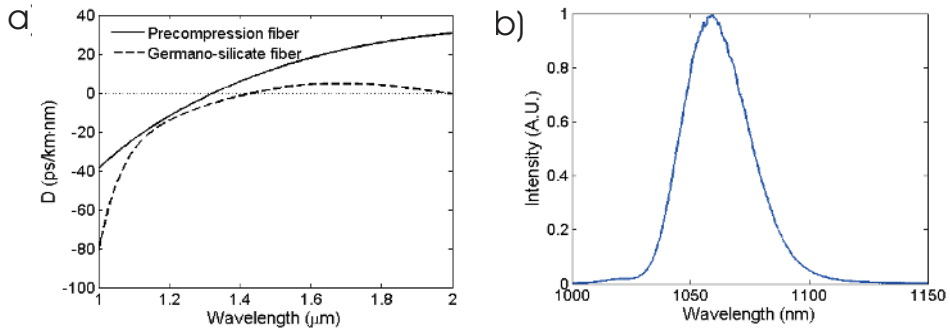

Fig. 2. Characteristics of the HNLF. On the left, the dispersion curves for the PF and for HNLF. On the right, spectrum around 1 μm at the output of the HNLF.

RBA30-1C2) where their energy is increased to 2.5 mJ.

The amplification at 1.6 μm is achieved using a two-stage OPCPA. The internal noncollinear angle is set to 3.2° to maximize the bandwidth of the stages [11]. The first stage consists of a 15-mm long potassium titanyl arsenate ($KTiOAsO_4$, KTA) crystal in a double-pass configuration while the second stage has a 10-mm KTA crystal in a single-pass configuration. Both stages share the same pump beam. KTA crystals are used because they offer a broad phase-matching in the infrared combined with a transparency window that goes from UV (350 nm) to the MIR (5000 nm). The seed and the pump have a beam diameter of 1.5 mm ($1/e^2$). The pump intensity in the first crystal is approximately 5 GW/cm^2. The seed power is 2.8 mW at 20 MHz (140 pJ per pulse). The power after the first, the second, and the third passes is 4.2 mW, 320 mW and 520 mW respectively. The amplified pulse energies are 1.4 μJ, 320 μJ and 520 μJ. The gain on the first pass is 10^4. On the second pass, the gain drops to 228 due to saturation. On the 3rd pass, the saturation effect is even stronger and the gain only reaches 1.625. For each stage, the super-fluorescence is measured by blocking the seed before the first crystal. After the first two stages, the super-fluorescence is negligible, whereas after the third stage it is 5 mW. This sets the background super-fluorescence upper limit to 1% as the super-fluorescence would be much weaker for the seeded OPA (due to the competition for the gain between the seed and the noise).

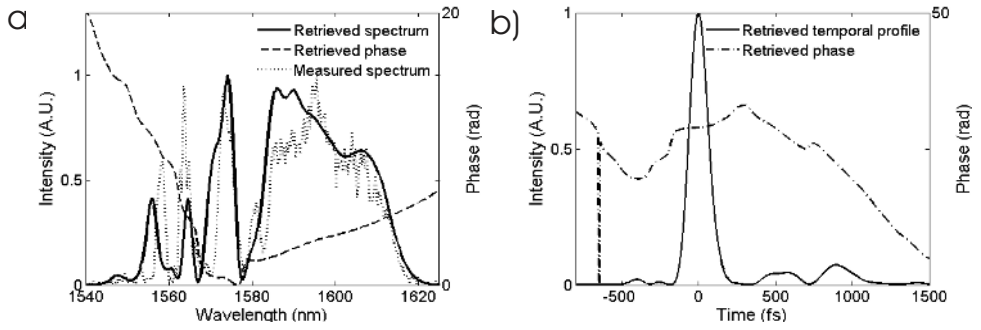

Fig. 3. Retrieved temporal electric field using a SHG-FROG. The pulse duration is estimated to be 140 fs.

#175727 - $15.00 USD Received 10 Sep 2012; revised 19 Oct 2012; accepted 23 Oct 2012; published 26 Nov 2012

The pulse-to-pulse stability is 1% (for 256 pulses), which is quite remarkable for an OPCPA. This level of performance is a major accomplishment of this work and is undoubtedly related to the effective elimination of the timing jitter in the seeding process (vide infra). The amplified pulses are recompressed using a reflective grating compressor (gold gratings, 750 lines/mm) and the output power after compression is 300 mW. After optimization of the compressor, the electric field of the pulse was characterized using a β-barium borate (BaB_2O_4 - BBO) second-harmonic FROG. Figure 3 shows the electric field in the time domain as retrieved from the FROG measurement. The pulse duration is about 140 fs with close to 75% of the energy within the main peak. Figure 3 also shows the retrieved and measured spectra; they are fairly broad and featureless above 1580 nm ,whereas below there is a series of sharp peaks. These two different behaviors can be explained by self-phase modulation (SPM) in the erbium-fiber amplifier. The input spectrum of the amplifier covers a region going from 1530 nm to 1590 nm. For strong SPM, the generation of new spectral components in the wings of the spectrum is associated to the appearance of modulations in the central region [22]; these are responsible for the peaks in the blue-side of the amplified spectrum as the OPCPA only amplifies part of the input. There is clearly a residual phase, which is strongly asymmetric, that could explain the relatively long pulse duration. The asymmetry seems to indicate that there is a strong contribution from both the second and third order phase, as they would add constructively on one side and destructively on the other. The compression is attributed to the extra-phase picked in the fiber amplifier from SPM and material dispersion, and pre-compensation with bulk material should be investigated as well as using gratings with a different groove density for the compressor [23] in order to improve the compression.

2.2. Timing jitter

The timing jitter was measured at the OPCPA position using cross-correlation between the pump and the seed pulses. The first KTA crystal was replaced by a 2-mm BBO crystal while keeping the same external noncollinear angle. The sum-frequency-generation (SFG) signal at 619 nm was monitored using a Si photo-diode. The time delay between the pulses was set to one of the half-maxima, where the SFG signal is linear with the delay. By recording the noise at this position, timing jitter can be extracted by measuring how the SFG signal changes with the delay, which is done by recording a full cross-correlation trace. The SFG noise was 1.1% (for 256 pulses), corresponding to 315 fs, which is less than 1% of the pump beam duration. This relatively small difference is attributed to thermal and cooling water induced acoustic effects in the YLF amplifier. The timing jitter between the seed and pump pulse is completely negligible compared to this source of jitter. The overall time jitter can be further reduced by temperature stabilizing and matching the regenerative amplifier cavity. Even without these modifications, the present timing jitter represents an exceptional level of passive stabilization with respect to the timing requirements for an OPCPA system.

3. Mid-infrared optical parametric amplifier

The OPA is based on a fairly novel crystal, lithium gallium selenide ($LiGaSe_2$ - LGSe), which has similar nonlinear coefficients, around 10 pm/V [24] , to Silver Gallium Sulfide ($AgGaS_2$ - AGS), the commonly used crystal in MIR generation. The interest in LGSe is partially fueled by its advantageous properties, e.g. higher thermal conductivity, and transparency down to 375 nm [24], but also by the low surface damage threshold of the AGS, which can be an order of magnitude lower than the bulk damage threshold [25]. Although, the damage threshold in LGSe was not formally investigated in this work, the crystal was able to handle higher intensity than the AGS crystal ($> 1.4\times$).

#175727 - $15.00 USD Received 10 Sep 2012; revised 19 Oct 2012; accepted 23 Oct 2012; published 26 Nov 2012

3.1. *Angular dispersion compensation*

The OPA is seeded by the idler of the OPCPA, which has an angular frequency chirp. It is possible to match this angular dispersion to the one of a grating by using a telescope, the resulting output being free of chirp [26].

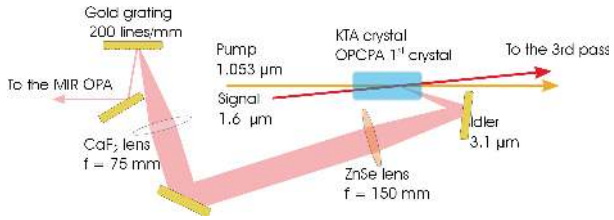

Fig. 4. The angular compensation setup. The idler is picked up after the second pass in the first crystal of the OPCPA.

With a telescope having a magnification of 1/2, the dispersion of a 200 lines/mm gold grating with an incident angle of 35° was used to remove most of the chirp in the idler (the detailed setup is shown in Fig. 4). This was investigated by dispersing the output using another grating, and by looking at the focal plane of a 150-mm cylindrical mirror placed at distance of 150 mm from the grating. This combination of grating/cylindrical mirror maps the spectrum with respect to the spatial coordinate associated with the spatial chirp; an unchirped beam will have its spectrum dispersed along the frequency axis, but aligned along the spatial axis. The results for the uncompensated and the compensated beams are shown in Fig. 5. By visual inspection it is clear that, although not perfect, most of the chirp was compensated for.

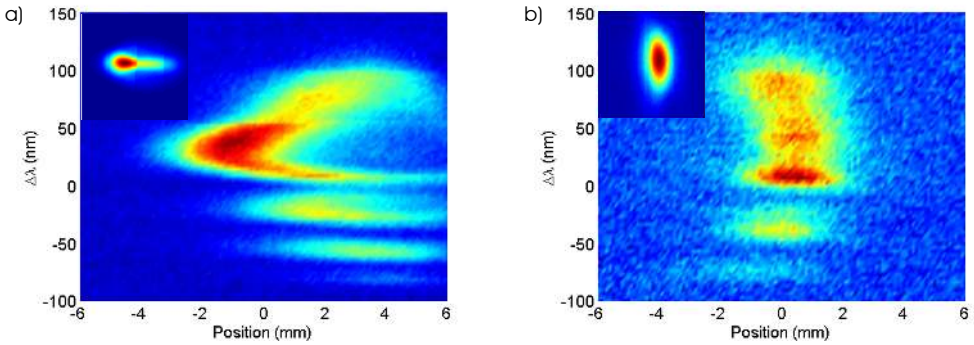

Fig. 5. Beam profiles at the focal plane of the cylindrical mirror. The vertical axis represents the spread in wavelength. For the uncompensated beam, on the left, the chirp is clearly visible, as the different frequencies have a different spatial position. For the compensated beam, on the right, there is still some chirp; however it is a lot less. The input profile of the beam is shown in the inset; the range for both axis is -3 mm to 3 mm.

3.2. *LGSe OPA*

The compensated idler provides the seed for the MIR-OPA. Because the idler is much longer than the pump, 50 ps vs 140 fs, no partial recompression using bulk material was attempted; an incomplete compression would result in a stronger pedestal in the signal. The OPA consists of a single 2-mm LGSe crystal in a single pass configuration and is pumped by the compressed

#175727 - $15.00 USD Received 10 Sep 2012; revised 19 Oct 2012; accepted 23 Oct 2012; published 26 Nov 2012

output of the OPCPA at 1.6 μm. As there is no real gain in bandwidth by using a noncollinear geometry, a small internal angle, 1.3°, was used to facilitate the separation of the different beams, while trying to minimize the angular dispersion of the idler. In this study, efficiency was the primary issue, and Type II phase-matching was used because it has a higher d_{eff} as well as a smaller group-velocity mismatch for the pump and the signal compared to Type I. The

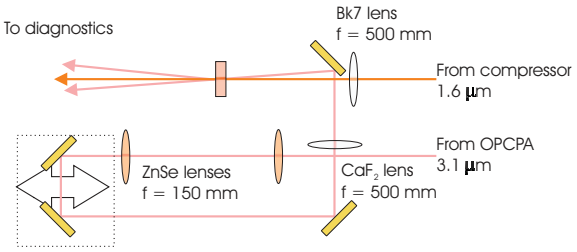

Fig. 6. MIR OPA setup.

MIR OPA setup is illustrated in Fig. 6. The spot sizes ($1/e^2$ diameter) at the crystal position are 1.44 x 2.06 mm^2 for the pump and 1.38 x 3.10 mm^2 for the seed. At this point the power in the 140-fs pump is 290 mW, resulting in a peak intensity of 172 GW/cm^2. The power in the seed before amplification is 4.6 mW for a 50-ps pulse at 1 kHz, which means that the energy of the seed overlapping the 140-fs pump pulse is about 16 nJ. After amplification the average power of the signal is 16.1 mW, an increase of 11.5 mW which represents an overall gain of 716 (compared to the seed energy overlapping the pump, 16 nJ). The power in the idler is 11.1 mW for a combined power of 22.6 mW, which corresponds to an overall efficiency of 8%. The pulse durations of both the signal and the idler were measured using an all-reflective autocorrelator (AC) based on two-photon absorption in an InGaS photo-diode. The autocorrelation traces as

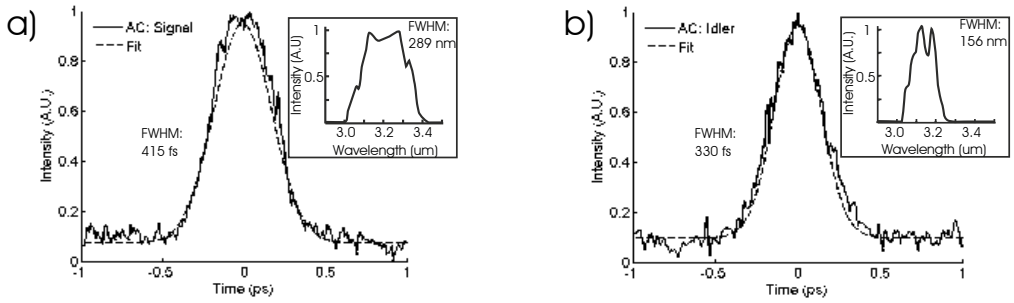

Fig. 7. MIR autocorrelation traces for the signal, on the left, and for the idler, on the right. From those traces, the retrieved FWMH pulse-width for the signal is 291 fs and 233 fs for the idler. The spectrum is shown in the inset.

well as the spectra are shown in Fig. 7. Although the OPA is operated near degeneracy, the spectrum of the idler is narrower than that of the signal. The difference in spectrum can be attributed to the broadband pump. Because the seed is stretched to 50 ps, it can be considered monochromatic when interacting with the 140-fs pump. Therefore, the pump will first generate a broadband idler that will then act as a source for the new signal frequencies, and because of phase matching, certain combinations of pump and idler frequencies will be favored over others. The FWHM bandwidth is 289 nm for the signal and is 156 nm for the idler, which

#175727 - $15.00 USD Received 10 Sep 2012; revised 19 Oct 2012; accepted 23 Oct 2012; published 26 Nov 2012

corresponds to a pulse duration of 52 fs and 97 fs for transform-limited (TL) pulses. From the traces, the pulse durations were estimated, using a Gaussian profile, to be 291 fs for the signal and 233 fs for the idler. The discrepancies can be explained by a few factors. First, because the pulse duration is 140 fs for the pump and 50 ps for the seed, the amplified pulses cannot be much shorter than the pump. Secondly, for the idler, the group-velocity mismatch is not zero; for a difference of group indexes of 0.031 between the idler and the pump, the propagation in a 2-mm crystal will introduce a relative displacement of 205 fs, which effectively stretches the idler. Finally, to avoid getting swamped by the 1.6 μm background, a 3-mm thick germanium plate was put before the detector in the AC; its dispersion is enough to stretch a 50-fs pulse to 260 fs and a 100-fs pulse to 160 fs.

The stability of the MIR was measured using two-photon absorption in an InGaAs photodiode. The photodiode signal had a standard deviation of 4.6% (for 256 pulses), putting a lower limit on the MIR stability at 2.3% for a shot-to-shot stability for the regen of 1.5% (for 256 pulses).

4. Conclusion

In summary, we have developed a highly robust, optically synchronized, OPCPA system that is based on robust fiber laser and readily scalable 1-μm amplifier technology. This system is used as the front end to cascade the fundamental output of the KTA-OPCPA at 1.6 μm to the MIR using a LGSe OPA tuned to 3.2 μm for comparative performance. For the OPCPA, the output power was 300 mW at 1 kHz repetition rate for pulses compressed to 140 fs. The all-optical synchronization based on a HNLF reduces the timing jitter to a usable 315 fs, limited only by opto-mechanical stability. There is only one oscillator in the system and it is a commercial fiber laser which improves the overall robustness of the setup and reduces the cost, especially compared to Ti:Sapphire systems. For the MIR OPA, the amplified output power is 11.6 mW for the 291-fs signal and 11.1 mW for the 223-fs idler. Although the efficiency is relatively low, the MIR power is already on par with most Ti:Sapphire-based OPAs. As the OPA is operated at degeneracy, the central wavelengths for the signal and the idler are around 3.2 μm, which is close to the frequency of a C-H stretch for applications in strong field control molecular systems. The OPCPA output and the MIR OPA tunability could be improved by using a HNLF in the seed arm of the OPCPA to produce shorter and cleaner tunable pulses at a longer wavelength. Furthermore, the power output of the OPCPA is only limited by the crystal aperture and the available pump power. With Nd-doped and Yb-doped systems capable of reaching 100 W to KW levels [27, 28], average output powers on the order of 10W at 1 kHz could be readily achieved at 1.6 um. This would result in millijoules of pulse energy over the entire MIR at a repetition rate and, equally important, stability that are interesting for spectroscopy and strong field control.

Acknowledgment

We would like to thank Dr. Darren Kraemer for helpful discussions and the suggestion to try LGSe crystals as a base for MIR generation. This research was supported by the Natural Sciences and Engineering Research Council of Canada.

#175727 - $15.00 USD Received 10 Sep 2012; revised 19 Oct 2012; accepted 23 Oct 2012; published 26 Nov 2012